Current Biology, Vol. 15, 2086–2096, December 6, 2005, ©2005 Elsevier Ltd All rights reserved. DOI 10.1016/j.cub.2005.11.016

Chemotaxis Behavior Mediated by Single Larval Olfactory Neurons in *Drosophila*

Elane Fishilevich,[1,4] Ana I. Domingos,[1,4] Kenta Asahina,[1] Félix Naef,[2,3] Leslie B. Vosshall,[1,*] and Matthieu Louis[1]
[1] Laboratory of Neurogenetics and Behavior
[2] Laboratory of Mathematical Physics
The Rockefeller University
1230 York Avenue
New York, New York 10021
[3] Computational Systems Biology
ISREC
Ch. des Boveresses 155
CH-1066 Epalinges
Switzerland

Summary

Background: Odorant receptors (ORs) are thought to act in a combinatorial fashion, in which odor identity is encoded by the activation of a subset of ORs and the olfactory sensory neurons (OSNs) that express them. The extent to which a single OR contributes to chemotaxis behavior is not known. We investigated this question in *Drosophila* larvae, which represent a powerful genetic system to analyze the contribution of individual OSNs to odor coding.
Results: We identify 25 larval *OR* genes expressed in 21 OSNs and generate genetic tools that allow us to engineer larvae missing a single OSN or having only a single or a pair of functional OSNs. Ablation of single OSNs disrupts chemotaxis behavior to a small subset of the odors tested. Larvae with only a single functional OSN are able to chemotax robustly, demonstrating that chemotaxis is possible in the absence of the remaining elements of the combinatorial code. We provide behavioral evidence that an OSN not sufficient to support chemotaxis behavior alone can act in a combinatorial fashion to enhance chemotaxis along with a second OSN.
Conclusions: We conclude that there is extensive functional redundancy in the olfactory system, such that a given OSN is necessary and sufficient for the perception of only a subset of odors. This study is the first behavioral demonstration that formation of olfactory percepts involves the combinatorial integration of information transmitted by multiple ORs.

Introduction

The olfactory system permits animals to detect, discriminate, and produce an appropriate behavioral response to a vast number of different odors. The first step in odor coding occurs at the periphery, where odor molecules interact with odorant receptor (OR) proteins that are expressed in olfactory sensory neurons (OSNs). ORs are seven-transmembrane-domain receptors that range in number from >1000 in mouse and *C. elegans* to <200 in insects [1]. Each OR is thought to interact with a number of odor ligands, and a given odor is thought to interact with multiple ORs, leading to a model of combinatorial odor coding in which odor identity is encoded by the activation of distinct groups of ORs [2–5]. Experimental support for this combinatorial-coding model of odor identity has been provided by functional imaging studies in diverse species [6–11]. Nonetheless, to what extent a single OR contributes to olfactory behavior is not known.

The larval stage of *Drosophila* is an excellent model system to test the influence of single ORs on chemotaxis behavior. Larvae have in two bilaterally symmetric dorsal organs only 21 OSNs [12, 13] that express at least 23 members of the *OR* gene family along with *Or83b*, an *OR* gene essential for olfaction [14–17]. The first olfactory synapse in the brain is organized into glomeruli [16, 18, 19], with a structure analogous to that of the vertebrate olfactory bulb. Larvae show strong odor-evoked chemotaxis behavior to a number of synthetic and natural stimuli [14, 20–23].

Here, we generate genetic tools that allow us to manipulate the functionality of the peripheral system of the larva by either ablating single OSNs or constructing larvae with one or two functional OSNs. This approach has allowed us to deconstruct sensory input to the olfactory system and to examine the individual contribution of identified OSNs to chemotaxis behavior.

Ablation of single OSNs reveals extensive functional redundancy in the larval olfactory system: A given OR is only necessary for chemotaxis to a small subset of odors tested. Animals with only a single functional neuron can chemotax robustly toward a number of odor stimuli. Combinatorial coding afforded by the entire ensemble of ORs is not strictly necessary for an animal to perceive and chemotax toward an odor. However, adding to a single-neuron animal a second functional OSN, which by itself is not sufficient to mediate chemotaxis, produces enhanced behavioral responses to a subset of odors. These results demonstrate at a behavioral level that a single OSN is sufficient to detect the presence of an olfactory stimulus and that the combinatorial activation of different ORs participates in the formation of olfactory percepts.

Results

Larval-Odorant-Receptor Gene Expression

The "nose" of the *Drosophila* larva resides in a pair of dorsal organs at the anterior tip of the animal, each containing 21 OSNs [13, 18] (Figures 1A–1B). Previous studies showed that up to 23 of the 61 *Drosophila* ORs are expressed in larvae by PCR and transgenic analysis [16, 17]. We performed RNA in situ hybridization to provide direct evidence that *OR* genes are expressed in larval OSNs. *Or83b*, which is necessary for the proper localization and function of conventional ORs [14, 15], is broadly expressed throughout the dorsal-organ ganglion [14] (Figure 1C). Twenty-four of the 30 *OR*s tested

*Correspondence: leslie@mail.rockefeller.edu
[4] These authors contributed equally to this work.

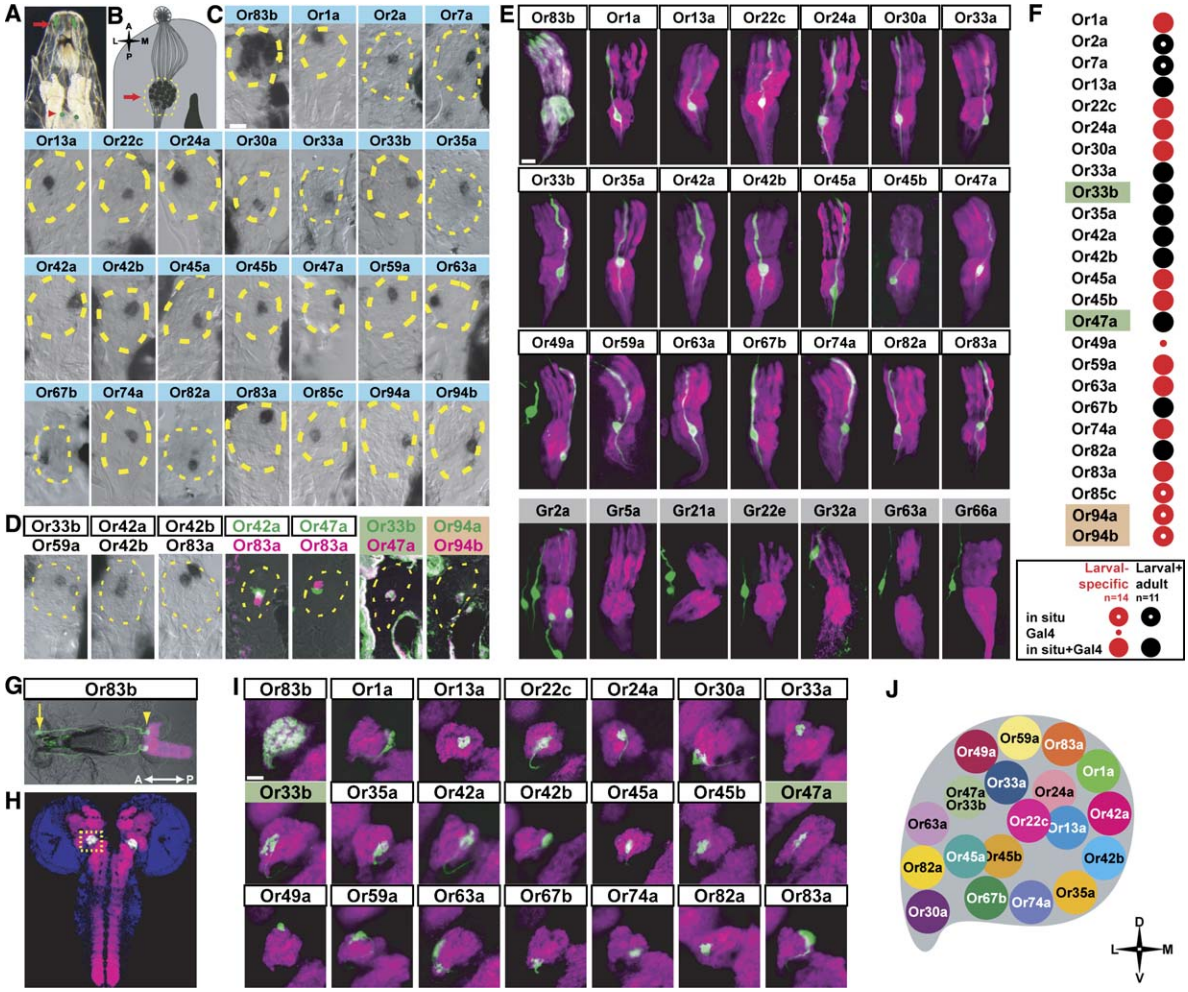

Figure 1. Molecular neuroanatomy of the Dorsal Organ of *Drosophila* Larvae

(A) Live imaging of GFP in a third-instar *Or83b*-Gal4;UAS-GFP animal. Dorsal-organ OSNs (red arrow) extend axons that innervate the larval antennal lobe (red arrowhead).

(B) Schematic diagram of the left dorsal organ with the cell-body ganglion indicated with the yellow dotted line. Red arrow is at the same relative position as in (A). The left mouth hook is shown at the bottom right. Orientation of samples in (B–E) is indicated at the left.

(C) RNA in situ hybridization shows that *Or83b* mRNA is broadly distributed in the larval dorsal organ and that expression of each larval *OR* is restricted to a single OSN. The border of the dorsal-organ cell-body ganglion is indicated by the yellow dotted line in each sample. Dark objects at the posterior-medial edge are the mouth hooks. Dark staining at the lateral edge is background labeling of the larval cuticle. The scale bar = 10 μm.

(D) RNA in situ hybridization with mixtures of two *OR* probes reveals five cases of nonoverlapping *OR* expression (left) and two cases of *OR* co-expression (right). The border of the dorsal-organ cell-body ganglion is indicated by the yellow dotted line in each sample.

(E) Whole-mount immunofluorescence staining of left larval dorsal organ of 21 different *OrX*-Gal4 driver lines crossed to UAS-GFP with *OrX*-Gal4::UAS-GFP transgenes in green and *Or83b*-Myc in magenta. *Or49a*-Gal4:UAS-GFP labels a single terminal-organ gustatory neuron in addition to a single dorsal-organ OSN. *GrX*-Gal4:UAS-GFP-positive neurons (green) are distinct from OSNs labeled with *Or83b*-Myc (magenta). The scale bar = 10 μm.

(F) Summary of larval *OR* gene expression with symbols at bottom of panel.

(G) Lateral view of the anterior tip of an *Or83b*-Gal4::UAS-GFP larva with dorsal-organ OSNs (green; yellow arrow) extending axons to the brain (yellow arrowhead), counterstained with the neuropil antibody nc82 (magenta). The animal is oriented anterior left, posterior right.

(H) Whole-mount immunofluorescence staining of an *Or83b*-Gal4::UAS-GFP larval brain with terminals of OSNs (green) in the larval antennal lobe (indicated by yellow dashed square, magnified in [C]). Counterstaining is nc82 (magenta) and a nuclear stain (TOTO-3; blue).

(I) Left antennal lobes of *OrX*-Gal4::UAS-GFP or UAS-CD8-GFP animals stained with GFP (green) and nc82 (magenta). The left larval antennal lobe is centered in the box, and the subesophageal ganglion is located at the lower right. The scale bar = 10 μm.

(J) Flattened representation of the larval-antennal-lobe glomerular map showing relative positions of glomeruli receiving input from an *OR*-expressing sensory neuron. Partially overlapping circles represent glomeruli whose position cannot be unambiguously resolved. Orientation of samples (I–J) is indicated at bottom right.

here are expressed in a single larval neuron in the dorsal organ (Figure 1C). We do not detect the expression of *Or10a*, *Or43b*, or *Or49a* mRNA or OR43b protein, although RT-PCR analysis detects these transcripts in larvae [16] (data not shown). *Or92a* and *Or98b* are also not detected by RNA in situ hybridization (data not shown). Most larval OSNs express a single *OR* along with *Or83b* (Figure 1D and Figure S1A in the

Supplemental Data available with this article online), but two OSNs coexpress a pair of *OR*s along with *Or83b*: *Or33b*/*Or47a* (Figure 1D, green) and *Or94a*/*Or94b* (Figure 1D, peach). Such *OR* coexpression has also been documented in the adult olfactory system [17, 24–26].

In parallel with the RNA in situ hybridization analysis, we examined a collection of 42 different *OR*-Gal4 transgenes that drive the expression of Gal4 [27] under the control of *OR* promoter elements [25, 28]. To visualize gene expression in the dorsal organ, we crossed individual *OR*-Gal4 lines to UAS-GFP, encoding cytoplasmic green fluorescent protein (GFP) and the olfactory-neuron marker *Or83b*-Myc. *Or83b*-Gal4 labels all 21 larval OSNs [14] (Figure 1E, green). Per dorsal organ, 19 of the remaining 41 *OR*-Gal4 transgenes label a single larval OSN (Figure 1E, green) that is also positive for *Or83b*-Myc (Figure 1E, magenta). Although we do not detect *Or49a* mRNA in larvae, *Or49a*-Gal4 labels one dorsal-organ OSN along with a single terminal-organ gustatory neuron (Figure 1E), consistent with a previous report [16]. Gustatory receptor (*GR*) genes are expressed in both olfactory and gustatory organs of the adult fly [29, 30]. *GR*-Gal4 transgenes are expressed only in the gustatory terminal organ or in nonolfactory dorsal-organ neurons that do not express *Or83b*-Myc (Figure 1E). We identify a total of 25 *Drosophila ORs* expressed in the larval dorsal organ and provide direct evidence that 24 of these *OR* mRNAs are expressed in situ. Of these, 14 are only expressed at the larval stage, whereas 11 are utilized by both larval and adult olfactory systems (Figure 1F).

Larval OSNs project axons to the larval antennal lobe of the brain (Figures 1G and 1H) [16, 18, 19]. Patterns of axonal projections to the larval antennal lobe were examined in larvae carrying each of 20 larval *OR*-Gal4 transgenes along with UAS-GFP or UAS-CD8-GFP (Figure 1I). Each *OR*-Gal4 line reveals a single labeled axonal arbor that terminates in an antennal-lobe glomerulus whose position is conserved between animals (Figures 1I and 1J; Figure S1B).

Larval Chemotaxis Responses to Synthetic and Natural Odor Stimuli

The availability of genetic tools that uniquely label 19 of the 21 larval OSNs allows us to manipulate the odor code by deconstructing the peripheral olfactory input and examining effects on behavioral output. Toward this end, we first established a chemotaxis assay of sufficient sensitivity to quantify differences in odor-evoked behavior. Chemotaxis of wild-type larvae was measured in response to 53 synthetic monomolecular odorants and three natural *Drosophila* attractants. The assay involves single-animal analysis in which the position of individual chemotaxing larvae is tracked over the course of a 5 min experiment [14]. The median of the mean distances to the odor calculated over several trials is represented by a pseudocolor scale from 0 (maximal attraction) to 8.5 cm (maximal repulsion) (Figure 2A). Distance to odor is used here as a measure of chemotaxis intensity with the assumption that the degree of attraction correlates inversely with the distance to the odor. The distribution of anosmic $Or83b^{-/-}$ and wild-type $Or83b^{+/+}$ larvae in space over the course of a 5 min experiment is represented by sector plots in Figure 2B. The 8.5 cm plate is divided into 21 sectors, and the average percent time an animal spends in each sector is plotted in grayscale (Figure 2B, left). Note that although anosmic $Or83b^{-/-}$ mutant (red) and wild-type $Or83b^{+/+}$ (cyan) larvae explore the plate in the absence of odor, only $Or83b^{+/+}$ larvae are strongly attracted to the sector containing the odor. As previously described, $Or83b^{-/-}$ larvae do not respond to odors [14].

We used this assay to screen larval chemotaxis to a panel of 53 synthetic odors and quantified the median distance to odor for $Or83b^{-/-}$ and $Or83b^{+/+}$ larvae (Figure 2C). Forty of these 53 odors are naturally present in fruit [23, 31–36] (Figure 2C, dots under apple symbol), and of these 40, 13 are known to elicit behavioral and electrophysiological responses in *Drosophila* [23, 35, 36] (Figure 2C, green dots under apple symbol). Anosmic $Or83b^{-/-}$ larvae do not respond to any odors, but wild-type (*yw*) larvae respond to many odors with strong chemotaxis.

We next asked how sensitive larvae are to odors by performing chemotaxis experiments at various odor concentrations. The responses to 1-hexanol are weak and not statistically different from anosmic controls for low dilutions (Figure 2D, left), whereas responses increase steeply between 0.02 μl and 0.2 μl doses and appear to reach a plateau for higher concentrations. We find no evidence that higher concentrations elicit repulsion (Figure 2E; data not shown). Response thresholds to heptanal and isoamyl acetate are one and two log orders, respectively, below that of 1-hexanol (Figure 2D, center and right; Figure 2E, top).

To test whether the weak responses observed for some odors at 2 μl (Figure 2C) could be explained by high detection thresholds, we further tested seven of these odors with 20 μl (Figure 2E, bottom). Under these conditions, 1-butanol and 2,3-butanediol elicit chemotaxis, whereas the remaining five odors do not. Thus the 2 μl stimulus dose elicits robust chemotaxis across a large group of different odors (Figure 2C), in accord with previous behavioral studies [37, 38].

Upon loading of an odorant stimulus in the closed-dish assay, the spatial distribution and average airborne concentration of this odor in the dish will be partly determined by the odor's vapor pressure. Vapor pressure is thus likely to affect the behavioral response observed for a particular odorant stimulus. In addition to this factor, we anticipate that the olfactory system of the larva may be differentially tuned to different stimuli. In the initial phases of this study, we found no clear correlation between the vapor pressure of a given odor and its corresponding behavioral efficacy (data not shown). We therefore decided to avoid any normalization of stimulus concentration and used the same quantity of odor (2 μl) for all 53 stimuli tested.

We examined whether chemotaxis elicited by single odors is comparable to that obtained with natural stimuli. Chemotaxis was measured in the same assay to banana mush, balsamic vinegar, and yeast paste at different concentrations. We find that attraction elicited by single synthetic odors is qualitatively similar to that obtained with natural odor blends and that the same steep threshold and stable plateau properties are seen for both stimulus types (Figure 2F and 2G).

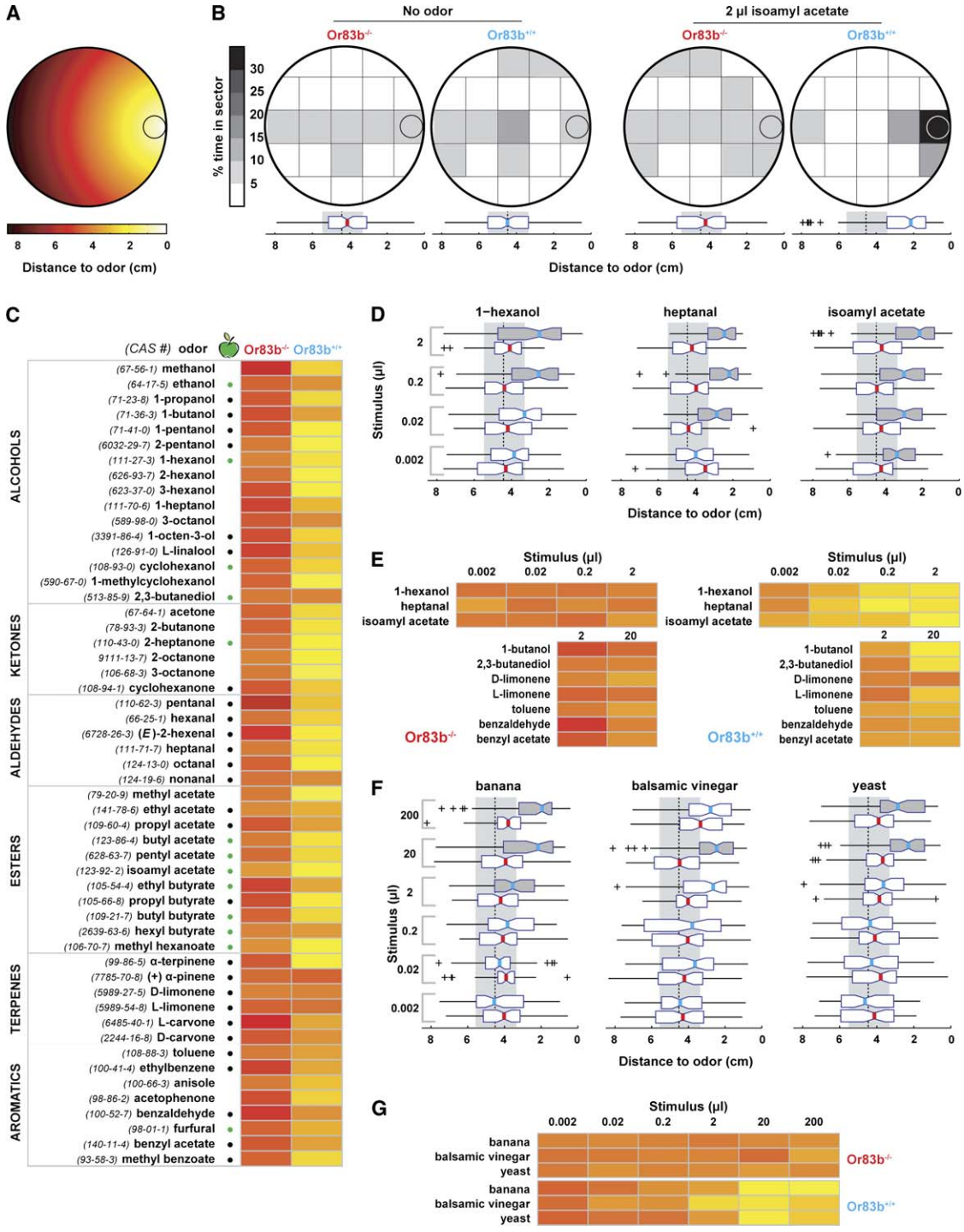

Figure 2. Larval Responses to Synthetic and Natural Odors

(A) Schematic of larval plate assay, pseudocolor coded for median distance to odor with the scale at bottom. Odor stimuli are placed on round filters located at the right edge of the plate, and distance relative to the odor is tracked during 5 min.

(B) Sector plots illustrating the averaged spatial distribution of larvae in response to no odor (left) or 2 µl isoamyl acetate (right), shaded according to the % time in sector scale at the left. Box plots indicating distribution of distances are under each sector plot. The median is indicated by the colored vertical line inside the box plot, box boundaries represent first and third quartiles, whiskers are 1.5 interquartile range, and outliers are indicated by hatch marks. We empirically established values corresponding to a neutral "no odor response" by measuring locomotor behavior of 110 wild-type (*yw*) animals on a plate containing no odor stimulus. The resulting value for the distribution of the mean distances to odor corresponds to a median of 4.45 cm, approximately the center of the plate (vertical black dashed line). The value of the first and third quartiles of the distribution is 3.30 cm and 5.50 cm, respectively (field of gray shading). Genotypes, left to right, are as follows: $Or83b^{1}/Or83b^{1}$, n = 111; *yw*, n = 111; $Or83b^{1}/Or83b^{1}$, n = 91; *yw*, n = 112.

(C) Responses of *Or83b* mutant (red) and wild-type (cyan) larvae to a panel of 53 synthetic odors presented at a dose of 2 µl. Black and green dots underneath the apple graphic indicate odors that are found in apple [32], cherimoya fruit [33], banana [34], or in at least three of 20 assayed

Genetic Ablation of Single Larval Olfactory Neurons

We next asked what the relative contribution of any given OSN to the formation of an odor percept is. Diphtheria toxin (DTI), an attenuated version of the cell-autonomous protein-translation inhibitor diphtheria toxin [39, 40], was used to ablate identified OSNs selectively. Most but not all larval OSNs are ablated by the expression of DTI along with GFP under control of the *Or83b*-Gal4 driver in all 21 larval OSNs. In *Or83b*-ablated animals, GFP expression is not detected (Figure 3A, left), and sensory dendrites are severely atrophied but not completely absent (Figure 3A, center). In *Or49a*-ablated animals, the *Or49a*-GFP marker is not visible (Figure 3A, right), and expression of other ORs is not perturbed (data not shown).

Chemotaxis of animals with single neurons ablated (*Or1a*, *Or42a*, or *Or49a*) was measured with a panel of 20 odors and compared to results obtained with the *Or83b*-ablation. To control for effects of genetic background, we compared the behavior obtained with each ablated animal to the corresponding parental controls. Nonparametric Wilcoxon rank-sum tests were performed to establish significantly impaired chemotaxis in ablated animals, correcting for multiple tests with the False Discovery Rate (FDR) method (see Experimental Procedures and Supplemental Experimental Procedures). Box plots for these experiments are presented in Figure S2. The summary plot in Figure 3B has been masked to show only those values with impaired chemotaxis that are statistically significant (see Figure S3A for an unmasked table). With this conservative statistical approach, *Or83b*-ablated larvae fail to respond to 17/20 odors (Figure 3B). If we allow for a single false discovery (FD), *Or83b*-ablated animals fail to respond to 19/20 odors. *Or1a*-ablated and *Or49a*-ablated animals each show reduced chemotaxis to a single different odor, (*E*)-2-hexenal and 1-hexanol, respectively, but show normal chemotaxis to the other 19 odors (Figure 3B). In contrast, ablation of the *Or42a* OSN causes decreases in chemotaxis to four of 20 odors. If we allow FD = 1, *Or1a*-ablated animals are impaired in responses to three of 20 and *Or42*-ablated animals to five of 20 odors (Figure S3B).

Behaviors Elicited by Sensing Odors with One Functional OSN

We next asked which OSNs are sufficient to produce chemotaxis to a given odor by constructing animals with only one or combinatorials of two functional OSNs. This was achieved by exploiting the *Or83b* mutation, which prevents OR trafficking to the sensory dendrite [14, 15, 41]. *Or83b* function was restored in individual OSNs by crossing animals with specific *OrX*-Gal4 drivers to UAS-*Or83b* animals, allowing us to assess the contribution of single neurons to odor-evoked behavior in the *OrX*-functional progeny.

Only a single OR83b-expressing neuron is seen in *Or42a*-functional, *Or49a*-functional, and *Or1a*-functional animals, whereas two OR83b-positive neurons are visible in *Or1a*-/*Or42a*-functional and *Or1a*-/*Or49a*-functional animals (Figure 4, top).The remaining OSNs are present but unlabeled in these animals because the *Or83b* mutation eliminates OR83b protein expression. We find no evidence that the glomerular map is distorted by the activation of a single OSN in a background of nonfunctional neurons as evidenced by the normal position and volume of the *Or1a* glomerulus in *Or1a*-functional and *Or83b* mutant larvae (Figure S6A).

These animals along with genetically matched control animals were screened for chemotaxis to 53 odors by using the same behavioral assay and nonparametric statistical analysis employed for the ablation experiments. Box-plot data are presented in Figures S4 and S5, and summary data for all 53 odors are in Figure 4 (bottom). The summary plot has been masked to show only those values with statistically significant chemotaxis allowing FD = 0 (see Figure S6B for an unmasked version of the table). The same data, allowing FD = 1 and FD = 2, are presented in Figure S6C. Consistent with the strong *Or42a*-ablated phenotypes (Figure 3B), *Or42a*-functional animals respond to 22 odors compared to 36 odors in $Or83b^{+/+}$ controls possessing 21 functional OSNs. *Or42a*-functional animals respond to three of four odors to which *Or42a*-ablated animals are anosmic (Figure 4). The broad behavioral response profile we observe for *Or42a*-functional larvae is in agreement with the broad ligand specificity of this OR as defined by electrophysiological experiments [16, 26].

In contrast to the broad odor response profile of *Or42a*-functional larvae, *Or1a*- and *Or49a*-functional animals do not show significant chemotaxis to any of the 53 odors tested, consistent with the weak phenotype of ablating either the *Or49a*-expressing or *Or1a*-expressing neuron (Figure 3B). These behavioral results are in accord with the ligand profiling of *Or49a*, which does not show strong electrophysiological responses to any of 27 odors tested [16].

varieties of mango [31]. Green dots indicate odors that were found to be relevant for flies via single-sensillum electrophysiological recordings in adult flies [35] or behavioral assays in adult flies [35, 36] or larvae [23]. Median distance to odor is expressed with the pseudocolor scale in (A). In total, 4780 larvae were tested; mean n = 45 (range 20–85) per odor and genotype. Chemical Abstracts Service (CAS) numbers for each odor are at left.

(D) Concentration dependence of larval odor responses. Significance was established by Wilcoxon rank-sum tests comparing data from $Or83b^{+/+}$ (cyan) to $Or83b^{-/-}$ controls (red) with Bonferroni correction for multiple comparisons. Box plots shaded dark gray indicate significant chemotaxis ($p < 0.05/4 = 0.0125$). In total, 1183 larvae were tested; mean n = 49 (range 30–64) per odor and genotype.

(E) Summary of concentration-dependent changes in larval behavior from (D), with the pseudocolor scale in (A), for anosmic $Or83b^{-/-}$ (red; left) and wild-type $Or83b^{+/+}$ larvae (cyan; right).

(F) Responses of $Or83b^{-/-}$ (red) and $Or83b^{+/+}$ (cyan) larvae to natural odor stimuli. Box plots shaded dark gray indicate significant chemotaxis with Bonferroni correction ($p < 0.05/6 = 0.0083$). In total, 2177 larvae were tested, mean n = 60 (range 36–67) per odor and genotype.

(G) Summary of natural-odor-evoked larval behavior from (F), with the pseudocolor scale in (A), for anosmic $Or83b^{-/-}$ (red; top) and wild-type $Or83b^{+/+}$ larvae (cyan; bottom). The highest dose of balsamic vinegar acidifies the agarose in the plate, attracting $Or83b^{-/-}$ larvae via their intact gustatory system (data not shown).

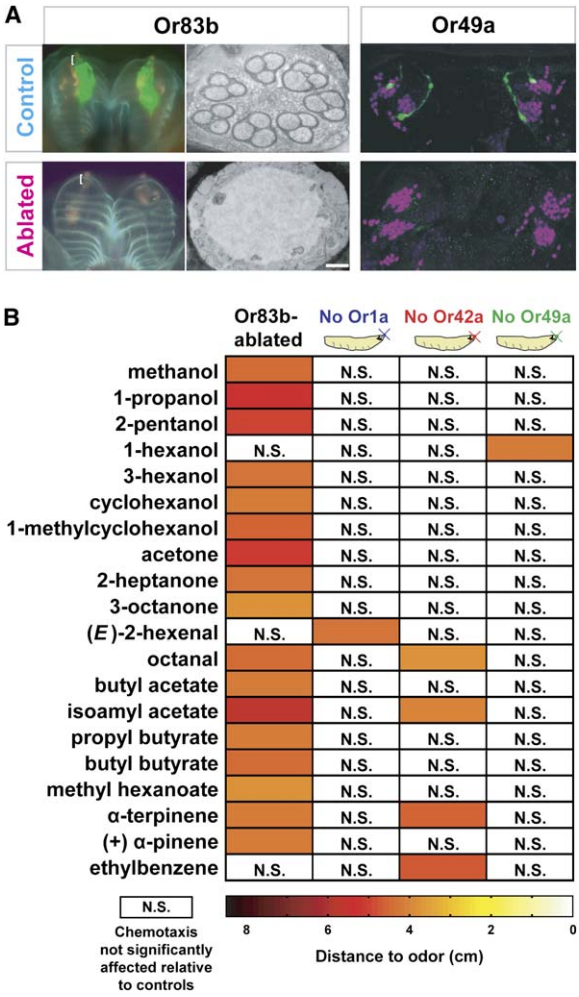

Figure 3. Genetic Ablation Reveals Extensive Redundancy in the Larval Odor Code

(A) Whole-mount GFP fluorescence (left; green) and thin-section electron micrographs (right) of *Or83b*-Gal4;UAS-GFP/TM6B larvae (top) and *Or83b*-Gal4;UAS-GFP/UAS-DTI larvae (bottom). Horizontal EM sections were obtained from the region indicated by the bracket in the left panels. The scale bar = 1 μm. Whole-mount GFP fluorescence (right, green) of *Or49*a-Gal4;UAS-GFP/TM6B larvae (top) and *Or49*a-Gal4;UAS-GFP/UAS-DTI larvae (bottom) is shown. Neuronal nuclei are labeled with ELAV (magenta).

(B) Summary of behavioral data to 20 odor stimuli presented at a dose of 2 μl. The difference in chemotaxis observed between the ablated genotypes and their parental controls was assessed upon adjustment of the nominal significance levels of Wilcoxon tests to maintain the family-wise type I error rate smaller than 0.05 (FDR method described in the Supplemental Experimental Procedures). For cases with significantly impaired chemotaxis relative to controls (level 0.05 allowing zero False Discoveries [FD]), distance-to-odor values are shown. All cases that do not meet this stringent statistical threshold are masked with a white box labeled N.S. (not significant; level 0.05 and FD = 0). Corrected nominal significance levels for each genotype are $p < 0.0029$ for *Or83b*, *Or1a*, and *Or42* and $p < 0.0028$ for *Or49a*.

Enhanced Chemotaxis Produced by Two Functional Olfactory Neurons

Although *Or1a*- and *Or49*-functional larvae do not chemotax to any odors tested, we asked whether these neurons contribute to chemotaxis in concert with the *Or42a* neuron. Chemotaxis performance of larvae with two functional neurons was compared to data from animals with only a single functional neuron. Larvae with two functional neurons respond to a somewhat different subset of odors than animals having either single functional neuron alone (Figure 4; Figures S4, S5, and S6).

To examine the existence of interactions between these neurons and identify cases of combinatorial enhancement, we developed a linear regression model to compare chemotaxis data across genetically matched controls for larvae with one or two functional OSNs (see Experimental Procedures and Supplemental Experimental Procedures). The model was designed to identify potential cases where single-neuron chemotaxis behavior differs from two-neuron behavior. The linear model suggests six cases of potential positive cooperativity between *Or1a* and *Or42a* chemotaxis that merited further experimental investigation (Figure S7). Additional chemotaxis experiments were carried out with four odors (1-pentanol, 2-pentanol, 2-hexanol, and 3-octanone) at three concentrations. 1-pentanol shows significantly stronger chemotaxis in *Or1a*/*Or42a*-functional animals than *Or42a*-functional or *Or1a*-functional animals at all three concentrations (Figure 5A). A qualitative view of this behavioral enhancement is seen in the sector-plot distributions comparing the anosmia of *Or83b* mutants (Figure 5B) to the progressive increase in chemotaxis to 1-pentanol of *Or1a*-functional or *Or42a*-functional compared to *Or1a*/*Or42*-functional (Figure 5C). The *Or1a*/*Or42*-functional animals spend comparatively more time in the sector containing the odor than animals having either single functional neuron alone. For the other three odors, this cooperative effect is significant at a single odor concentration (Figure S8).

Discussion

In this study, we use behavioral analysis to measure the contribution of individual neurons to the odor code and provide a missing link between our understanding of the molecular biology of ORs, the neurophysiological properties of the olfactory network, and complex odor-evoked behaviors. Our goal was to approach the question of how the combinatorial activation of ORs encodes odor stimuli and elicits olfactory behavior. Our results suggest that there is a high level of redundancy in the larval olfactory system, such that ablating a single neuron has minimal effects on odor detection. Among these olfactory inputs, the *Or42a* neuron plays a more important role in odor detection than the *Or1a* or *Or49a* neuron. Animals engineered to have the *Or42a* neuron functional are able to chemotax to multiple odors. The addition of a second OSN to such animals results in enhanced chemotaxis for several odors. Whereas *Or1a*-functional animals show no significant responses to any odor tested, we observe that responses of *Or1a*/*Or42a*-functional animals to four odors are enhanced relative to *Or42a*-functional animals. This suggests that although olfactory input contributed by the *Or1a*-expressing OSN is not sufficient alone to elicit robust chemotaxis, it enhances the perception of odors in conjunction with the information transmitted by the *Or42a*-expressing OSN. These behavioral results are summarized in schematic form in Figure 6.

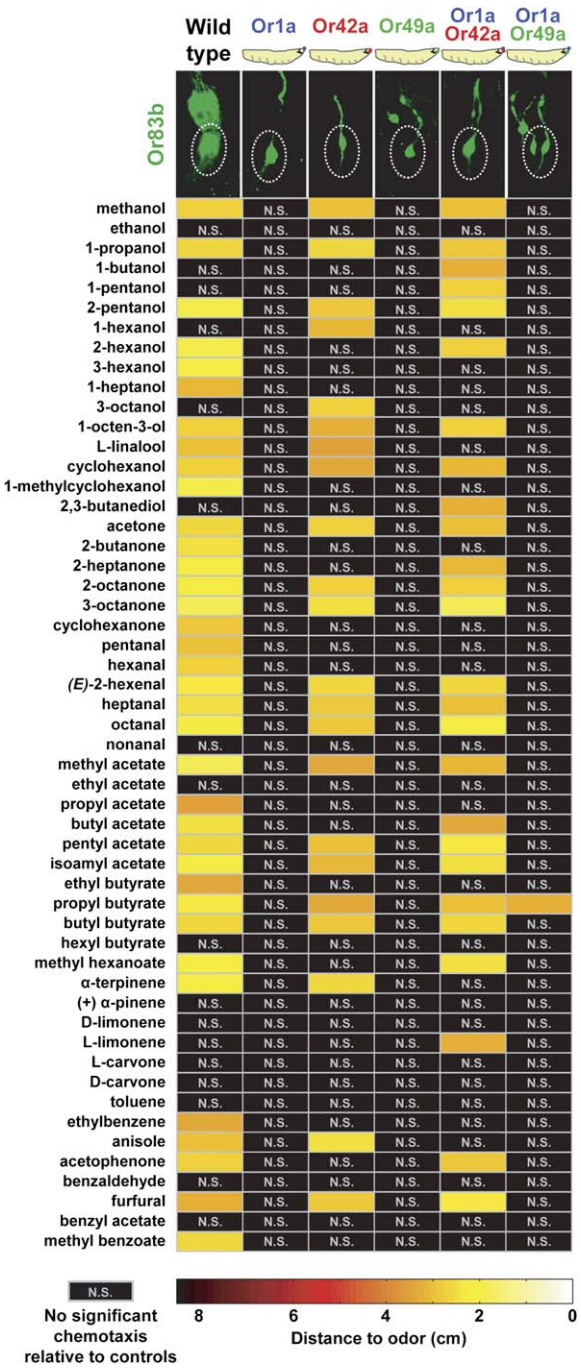

Figure 4. Chemotaxis Produced by Single Functional Olfactory Neurons

(Top) Schematic of larvae having single or pairs of functional OSNs. Immunofluorescence of OSNs stained with anti-Or83b antibody (green) (left to right): (1) *yw*, (2) *Or42a*-Gal4/UAS-*Or83b*;*Or83b*^{1}/*Or83b*^{1}, (3) *Or49a*-Gal4/UAS-*Or83b*;*Or83b*^{1}/*Or83b*^{1}, (4) *Or1a*-Gal4/UAS-*Or83b*;*Or83b*^{1}/*Or83b*^{1}, (5) *Or42a*-Gal4, *Or1a*-Gal4/UAS-*Or83b*;*Or83b*^{1}/*Or83b*^{1}, and (6) *Or49a*-Gal4, *Or1a*-Gal4/UAS-*Or83b*;*Or83b*^{1}/*Or83b*^{1}. White dotted line indicates boundary of dorsal-organ cell-body ganglion, as visible in the *yw* genotype. The terminal-organ neuron expressing *Or49a*-Gal4 is visible outside of the boundary of the dorsal organ.

(Bottom) Summary of behavioral data to 53 different odor stimuli, presented at a dose of 2 μl. Cases with significant chemotaxis (level 0.05; FD = 0) relative to anosmic controls show the distance to odor with the scale at bottom. All cases that do not meet this stringent statistical threshold are masked with a black box labeled N.S. (not significant at level 0.05 and FD = 0). In total, 29,235 larvae were tested, mean n = 50 (range 20–146) per odor and genotype. Corrected nominal significance levels for each genotype are $p < 0.0012$ for *Or83b* and $p < 0.0011$ for the remaining five genotypes.

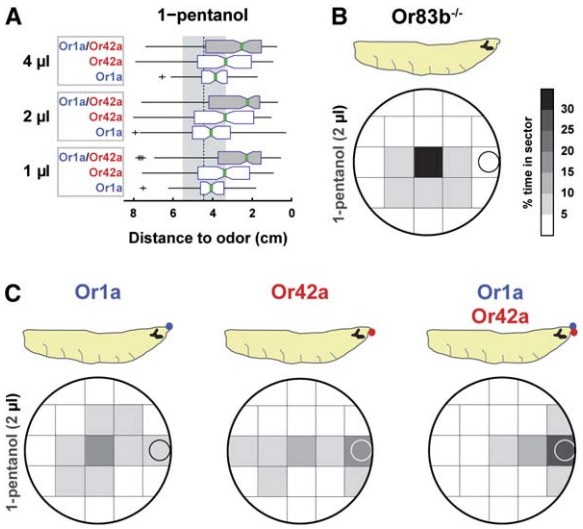

Figure 5. Combinatorials of OSNs Enhance Chemotaxis

(A) *Or1a*/*Or42a*-functional larvae exhibit enhanced chemotaxis to 1-pentanol compared with those having either single functional neuron alone. Box plots show chemotaxis data collected with 4 μl, 2 μl, or 1 μl of stimulus. Significance was established by Wilcoxon rank-sum tests comparing data from the double functional neuron larvae and the best single functional neuron larvae with Bonferroni correction for multiple comparisons ($p < 0.05/3$) (see also Figure S8).

(B) Sector plot showing the averaged spatial distribution of *Or83b*$^{-/-}$ animals in response to 2 μl 1-pentanol, plotted according to the scale at right.

(C) Sector plots showing the averaged spatial distribution of animals from (A) for 2 μl 1-pentanol with the scale in (B).

Behavior is the ultimate output of a sensory system that integrates all aspects of external-information processing. Our experiments demonstrate the feasibility and value of integrating behavioral analysis into the study of odor coding. We propose that the simple olfactory system of *Drosophila* larvae will be an invaluable model in any attempt to correlate the cellular basis of the odor code with its behaviorally relevant output.

The Larval-Odorant-Receptor Repertoire and Implications for Behavior

Drosophila is a holometabolous insect that undergoes dramatic changes in lifestyle from the larval to adult stage. In a sense, these animals can be considered to occupy completely separate ecological niches. Larvae maintain constant contact with food until pupation [42, 43], whereas adults are flying insects that use their sense of smell to identify suitable food sources and appropriate sites for egg-laying [36]. In essence, larvae are specialized for feeding and growth, whereas adults are devoted to breeding and dispersal. To what extent have these two life stages of the same species evolved a different chemosensory system? We show here that 14 of 25 larval *OR* genes are stage specific and not used again by the adult animal. All larval OSNs are

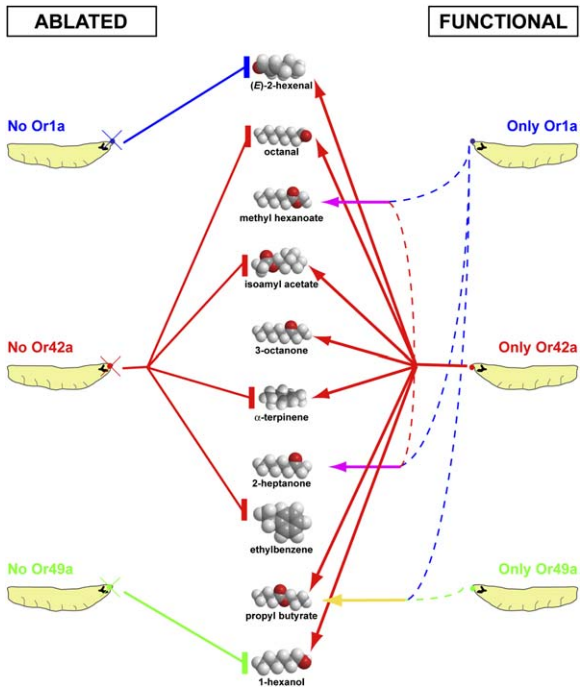

Figure 6. Larval Chemotaxis Behavior Is Integrated across Multiple ORs

This schematic diagram outlines the general conclusions we draw from our behavioral observations. At left, we indicate that specific OSNs are necessary for chemotaxis to a subset of odors (lines ending in vertical bars) in the context of an animal with one OSN ablated but retaining function in the 20 remaining OSNs. At right, we indicate that single OSNs and combinations of OSNs are sufficient to mediate chemotaxis in an animal having only those neurons functional (lines ending in arrows). This schematic includes data from Figures 3 and 4 and highlights that *Or42a* is both necessary and sufficient for chemotaxis to several odors. *Or1a* and *Or49a* are necessary for wild-type chemotaxis to a single odor each and are sufficient only in concert with another functional OSN. Responses to methyl hexanoate, 2-heptanone, and propyl butyrate require combinatorials of two functional OSNs, indicated by dashed lines merging into a solid line with a new color.

histolyzed in metamorphosis and replaced in the adult by newly differentiated antennal and maxillary palp OSNs [12]. Perhaps this developmental changeover has led to largely separate *OR* genes with transcriptional regulatory regions specific for either larval or adult olfactory organs. Alternatively, the segregation of larval- and adult-expressed *OR*s could be functional and relate to the different ecological niches that these life stages occupy: Larvae may cope with much higher odor concentrations because of their direct contact with food.

Implications for Central-Circuit Olfactory Coding

Odor processing occurs at various levels in the nervous system, from peripheral sensory neurons to primary processing centers, such as the olfactory bulb in vertebrates and the antennal lobe in insects, and further to higher brain centers of the olfactory cortex in vertebrates and mushroom body and lateral horn in insects. How the combinatorial code established by the ORs at the periphery is transmitted through this olfactory circuitry to produce the perception of an odor in any species is unknown. Our data support the notion that peripheral sensory neurons constitute information channels that are not independent but subject to interactions in the olfactory circuit. Otherwise, one would expect that the behavioral response profile observed for the *Or1a/Or42a*-functional genotype be given by the union of the best performances of the single *Or1*a- and *Or42a*-functional genotypes. Where and how the information is processed remains unclear, but part of this transformation may occur in the antennal lobe [44].

Clarifying the principles of Larval Odor Coding

A number of conclusions about odor coding in the *Drosophila* larva can be drawn from this work. There appears to be no clear structural relationship between the odors that elicit chemotaxis mediated by a given OSN, as has been previously shown in an analysis of the ligand response properties of ORs in the adult fly [5]. The *Or42a*-expressing neuron differs from other neurons studied here in the large number of odors that attract animals having only this neuron active. Interestingly, the behavioral response profile of the *Or42a*-functional genotype indicates that an OR may not need to be strongly activated by a given odor to allow for chemotaxis toward the odor source. This point is best illustrated by 3-octanol and anisole, which both elicit strong chemotaxis in *Or42a*-functional animals whereas they seem to induce relatively weak electrophysiological activity [16].

Finally, the behavioral receptive field of animals having combinatorials of functional neurons cannot be predicted from a simple model where the responses of animals having either single OSN functional are added. The chemotaxis results we report here highlight the existence of strong nonlinearities in the processing of olfactory information in such a way that in the arithmetic of sensory coding, the whole is greater than what the parts can produce independently. Such a scheme would be consistent with the extraordinary needs of the olfactory system to detect numbers of odors that greatly exceed the number of *OR* genes in any given animal. The functional redundancy we observe here could buffer the olfactory system against mutations and allow animals to adapt to changing or new odor environments.

Conclusions

The genetic tools presented here should permit a systematic analysis of the peripheral and central components that generate an odor response in the *Drosophila* larva. A number of key unanswered questions remain for future studies. Electrophysiological or optical imaging tools must be used to analyze the neuronal correlates of the behavior observed here. Greater understanding of the second- and third-order neurons that communicate information from the antennal lobe to eventual motor output is needed. This study has been restricted to simple chemotaxis assays, and no attempt has been made to query larvae for their powers of odor discrimination. Animals missing a single OSN may chemotax normally but experience olfactory-perception not uncovered in these chemotaxis assays. By coupling associative learning of odors in intact animals [45] followed by generalization tests in the same animals that conditionally lack a single OSN, it should be possible to

determine whether odor salience is altered in larvae missing a single OSN. Finally, it will be important to determine whether the phenomena reported here can be considered general olfactory-coding principles that also apply to more complex animals.

Experimental Procedures

Drosophila *Stocks*

All fly stocks were maintained on conventional cornmeal-agar-molasses medium under a 12-hr-light:12-hr-dark cycle at 18ºC or 25ºC. Transgenic constructs were injected into *yw* embryos with standard procedures and single transformants outcrossed to autosomal balancers for chromosomal mapping. The following fly stocks were kindly provided: UAS-GFP (Bloomington Stock Center), UAS-CD8-GFP (L. Luo), UAS-DTI14 (L. Stevens), and Gr-Gal4 lines (K. Scott and H. Amrein).

Generation of Transgenes Containing Odorant-Receptor Promoter Elements

OR regulatory sequences were obtained by long-range PCR with the Expand High Fidelity PCR System (Roche) on *Drosophila melanogaster* Oregon R genomic DNA, as described [28]. Reverse primers were placed immediately upstream of the predicted ATG initiation codon, and forward primers were at the following distances upstream: *Or1a*, 6.285 kb; *Or13a*, 8.199 kb; *Or22c*, 7.156 kb; *Or24a*, 8.72 kb; *Or30a*, 9.148 kb; *Or33a*, 5.155 kb; *Or33b*, 8.086 kb; *Or35a*, 3.88 kb; *Or42a*, 4.184 kb; *Or42b*, 8.039 kb; *Or45a*, 9.556 kb; *Or45b*, 4.764 kb; *Or47a*, 8.239 kb [28]; *Or49a*, 3.799; *Or59a*, 7.8 kb; *Or63a*, 4.205 kb; *Or67b*, 2.74 kb; *Or74a*, 7.226 kb; *Or82a,* 1.865 kb; *Or83a*, 1.628 kb; and *Gr63a*, 2.635 kb. The PCR products were cloned into pGEM-T Easy and then, after end-sequencing, subcloned into pCaSpeR-AUG-Gal4 as described [28].

Multiple independent transgenic lines were generated for each construct, and all were analyzed for expression in the larva. To detect Gal4 expression in dorsal organs, we crossed OrX-Gal4 flies to *Or83b*-Myc;UAS-GFP flies. To detect Gal4 expression in larval brains, we crossed OrX-Gal4 flies to UAS-GFP or UAS-CD8-GFP flies. There was some inter-line variability in the number of cells labeled in the dorsal organ and the occasional labeling of terminal organ or other nonsensory cells in the larva. Where this ectopic expression was not supported by in situ results, such lines were not used for behavioral analysis, with the exception of *Or49a*-Gal4, whose expression was not detected by RNA in situ. *Or98b*-Gal4 (5.12 kb) did not express, and *Or85c*-Gal4 (7.588 kb) showed ectopic expression. For *Or30a*-Gal4, there were reliably two additional cells of unknown function at the midline, posterior to the mouth hooks. *Or24a*-Gal4 is expressed in the adult maxillary palp, although *Or24a* mRNA is not detected in this tissue (data not shown). The following 21 adult *OrX*-Gal4 lines do not express in larval OSNs: *Or19a*, *Or22a*, *Or23a*, *Or33c*, *Or43a*, *Or46a*, *Or47b*, *Or49b*, *Or56a*, *Or59c*, *Or65a*, *Or67d*, *Or69a*, *Or71a*, *Or83c*, *Or85a*, *Or85e*, *Or85f*, *Or88a*, *Or92a*, and *Or98a*.

Or83b-Myc contains 7.76 kb of genomic DNA upstream of the *Or83b* initiation codon fused to the full-length *Or83b* cDNA (Genbank accession number AY567998). The cDNA was modified by mutating the stop codon and fusing DNA sequences encoding 5 Myc epitopes (MEQKLISEEDLNE) to the 3′ end. This DNA sequence was then ligated to the endogenous 3′ UTR of *Or83b* and the SV40 polyadenylation sequences. The DNA was cloned into pCasper4PLX, a CaSpeR vector modified to contain rare-cutting restriction enzymes. The *Or83*-Myc protein does not rescue the *Or83b* mutant phenotype (data not shown), but serves here as a pan-OSN marker.

In Situ *Hybridization*

Wild-type (Oregon-R) third-instar larvae were decapitated in 1× PBS and carefully dissected to remove the digestive tube posterior to the esophagus, the salivary glands, and fat body. The larval heads were then transferred to plastic embedding molds containing Tissue-Tek OCT, and they were aligned so that the dorsal side faced the bottom surface. The samples were frozen, and 12 μm frozen sections were processed for in situ hybridization as previously described [46]. Anti-sense DIG riboprobes were transcribed from *OR* templates derived from genomic DNA [28]. Twelve of the 61 *OR* genes were not examined in this study (*Or9a*, *Or19b*, *Or22b*, *Or46b*, *Or59b*, *Or65b*, *Or65c*, *Or67a*, *Or67c*, *Or69b*, *Or85b*, and *Or85d*), so the "complete" repertoire of larval *OR* genes may be slightly higher than the 25 described here. For double in situ hybridization, DIG probes corresponding to two *OR* genes were mixed in the same hybridization buffer. Sections were examined with Nomarski optics, which permitted identification of the dorsal-organ ganglion by its characteristic position and morphology. Two-color in situ hybridization was performed as previously described [46] with digoxigenin- (magenta) and fluorescein-labeled (green) riboprobes, detected first with TSA-Plus Fluorescein System (fluorescein; Perkin Elmer) and then with TSA-Plus Cyanine 5 System (digoxigenin; Perkin Elmer), after quenching the fluorescein reaction for 1 hr with 3% hydrogen peroxide. Anti-digoxigenin-POD and anti-fluorescein-POD were diluted 1:500 (Roche).

Immunofluorescence

Antibody staining of late third-instar larvae was performed as described [18] with primary antibodies (rabbit anti-GFP [Molecular Probes], mouse anti-Myc 9E10 [1:10; S. Morton, Jessell Lab-Columbia University], mouse anti-Elav 9F8A9 [1:10 dilution; DSHB, University of Iowa], mouse nc82 [1:10; R., University of Fribourg], and rabbit anti-Or83b [1:5000]) and secondary antibodies (1:100; CY3: Jackson ImmunoResearch; Alexa488: Molecular Probes). Nuclei were counterstained with a 1:1000 dilution of TOTO-3 (Molecular Probes). Larval brains were mounted with 11 × 22 mm No. 1 coverslips as spacers. Confocal Z-series with 0.45 μm thick sections that span GFP signal were collected with a Zeiss LSM510 confocal microscope.

Electron Microscopy

Anterior tips of *Or83b*-Gal4;UAS-GFP and *Or83b*-Gal4;UAS-DTI/UAS-GFP larvae were fixed in ice-cold 3% glutaraldehyde in 0.1 M cacodylate, pH 7.4, and dissected to remove all tissue posterior to the mouth hooks. Samples were postfixed in 1% osmium tetroxide and dehydrated in a graded alcohol, propylene oxide series and embedded in Durcupan resin. Pale-gold ultrathin serial sections were collected and post stained with uranyl acetate and lead citrate. Images were collected on a JEOL100CX electron microscope operated at 80 kV. Two animals of each genotype were analyzed in detail.

Larval Chemotaxis Assay and Statistical Analysis

Larval behavioral assays were carried out as described [14]. Odor stimuli (2, 4, or 20 μl neat or smaller quantities diluted in paraffin oil) were pipetted onto a filter placed inside a plastic cap located at one side of the Petri dish. Experiments in Figures 3 and 4 used a stimulus strength of 2 μl of neat odor because this elicits strong chemotaxis responses across a broad range of structurally different odors (Figure 2C) [21, 37, 38]. All odorants were supplied by Sigma-Aldrich and were of the highest purity available. Natural odors were commercial balsamic vinegar used at full strength or diluted in water, a liquid paste of 50% w/v ripe banana mush in water, and 20% w/v paste of activated baker's yeast in water. Single third-instar larvae were transferred to the plate, and their locomotor movement was videotaped for 5 min. The animal's X-Y coordinate was tracked at a sampling rate of 6 frames/s with EthoVision Pro (Noldus) tracking software. The assay was multiplexed, with 12 individual larvae assayed simultaneously in separate 85 mm circular arenas. Each animal was assayed only once with a single stimulus. We minimized the presence of air flow in these experiments by conducting the assay in Petri dishes with closed lids. Animals were tested within a few seconds of odor application.

Data were exported from Ethovision and analyzed with Matlab (The Mathworks) with a custom-written batch script. To filter out experiments with technical noise due to light scattering or tracking failures, any tracks shorter than 270 s or with a mean velocity = 0 cm/s or > 0.2 cm/s were discarded. All tracks that met these criteria were included in the statistical analysis and plotted in Figures 2–5 and Figures S2–S8. Larval chemotaxis behavior was quantified as the distance of the animal from the odor (Figure 2A). Distances recorded every second were averaged over the 5 min trial.

Unless indicated otherwise, all statistical analysis was performed with one-tailed nonparametric Wilcoxon rank-sum tests to measure differences between control and experimental data sets. For data in Figures 3 and 4 and Figures S3 and S6, each ablated or *Or83b*-rescued genotype was compared to its parental lines. We denote the ablated genotypes as follows: (α_1) *Or83b*-Gal4/+;UAS-DTI/+; (α_2) *Or1a*-Gal4/+;UAS-DTI/+; (α_3) *Or42a*-Gal4/+;UAS-DTI/+; and (α_4) *Or49a*-Gal4/+:UAS-DTI/+. The rescued genotypes are denoted as follows: (ρ_1) *Or1a*-Gal4/UAS-*Or83b*;*Or83b*^{1}/*Or83b*^{1}; (ρ_2) *Or42a*-Gal4/UAS-*Or83b*;*Or83b*^{1}/*Or83b*^{1}; (ρ_3) *Or49a*-Gal4/UAS-*Or83b*;*Or83b*^{1}/*Or83b*^{1}; (ρ_4) *Or42a*-Gal4, *Or1a*-Gal4/UAS-*Or83b*;*Or83b*^{1}/*Or83b*^{1}; and (ρ_5) *Or49a*-Gal4,*Or1a*-Gal4/UAS-*Or83b*;*Or83b*^{1}/*Or83b*^{1}. The genotypes used for controls are as follows: (η_1) UAS-DTI; (η_2) *Or83b*-Gal4; (η_3) *Or1a*-Gal4; (η_4) *Or42a*-Gal4; (η_5) *Or49a*-Gal4; (η_6) *Or83b*^{1}/*Or83b*^{1}; (η_7) UAS-*Or83b*/UAS-*Or83b*;*Or83b*^{1}/*Or83b*^{1}; (η_8) *Or1a*-Gal4/*Or1a*-Gal4;*Or83b*^{1}/*Or83b*^{1}; (η_9) *Or42a*-Gal4/*Or42a*-Gal4;*Or83b*^{1}/*Or83b*^{1}; and (η_{10}) Or49a-Gal4/Or49a-Gal4;*Or83b*^{1}/*Or83b*^{1}. In Figure 3 and Figure S3, comparisons were performed according to the following pairs of genotypes $\leftrightarrow$ controls: $\alpha_1 \leftrightarrow \{\eta_1, \eta_2\}$, $\alpha_2 \leftrightarrow \{\eta_1, \eta_3\}$, $\alpha_3 \leftrightarrow \{\eta_1, \eta_4\}$, and $\alpha_4 \leftrightarrow \{\eta_1, \eta_5\}$. In Figure 4 and Figure S6, comparisons were made according to the following: *yw* $\leftrightarrow \{\eta_6\}$, $(\rho_1) \leftrightarrow \{\eta_7, \eta_8\}$, $(\rho_2) \leftrightarrow \{\eta_7, \eta_9\}$, $(\rho_3) \leftrightarrow \{\eta_7, \eta_{10}\}$, $(\rho_4) \leftrightarrow \{\eta_7, \eta_8, \eta_9\}$, and $(\rho_5) \leftrightarrow \{\eta_7, \eta_8, \eta_{10}\}$. To address the problem of multiple testing, we have used a permutation-resampling-based technique to adjust the nominal p values and to keep the family-wise error rate to 0.05 everywhere [47]. The approach we implemented allows us to control the False-Discovery Rate (FDR) among the set of null hypotheses rejected by the Wilcoxon tests. This approach consists in a generalization of the Bonferroni correction procedure [47, 48] but accounts for possible non-independence of the tests. When the FDR is chosen as zero, the stringency of the two approaches is essentially equivalent given the low level of dependency between tests for different odors. See Supplemental Experimental Procedures for a detailed explanation of how the FDR control procedure was applied to this data set.

In Figure 5, we tested the existence of combinatorial interactions between individual neurons based upon a multiple regression model [49]. The mean distance separating a larva from the odor was described by the linear model

$$d_i = \beta_0 + \beta_1 . \Gamma_{\text{one OR}} + \beta_2 . \Gamma_{\text{two ORs}} + \varepsilon_i$$

where d_i denotes the distance of the i^{th} specimen to a given odor; ε_i is the i^{th} residual; and $\Gamma_{\text{one OR}}$ and $\Gamma_{\text{two ORs}}$ are binary indicators equal to 1 when the genotype has at least one or two functional neuron(s), respectively. Potential cases of synergism are related to significant increases in attraction: They are associated with values of $\beta_2 < 0$. Conversely, potential cases of inhibition are related to significant decreases in attraction: They are associated with values of $\beta_2 > 0$. We estimate the regression coefficients β_0, β_1, and β_2 by the least-squares method. The double-neuron functional data are compared to those of the single-neuron functional data characterized by the highest attraction. The "intercept" β_0 was computed with a merged subset of relevant negative controls (see Supplemental Experimental Procedures). To test whether the estimates of β_2 were significantly different from zero, we used two-tailed t tests with a significance level of 0.05.

Supplemental Data

Eight figures and Supplemental Experimental Procedures and can be found with this article online at http://www.current-biology.com/cgi/content/full/15/23/2086/DC1/.

Acknowledgments

We thank Susan Morton, Reini Stocker, and DHSB/NICHD (University of Iowa) for antibodies; Hubert Amrein, Liqun Luo, Kristin Scott, Leslie Stevens, and the Bloomington Stock Center for fly strains; Tanya Rogoff, Jeremy Fenton, Mana Mirjany, Austen Gess, Katie Belfi, and Lylyan Salas for expert technical assistance in molecular biology and genetics; Silvia Vasquez for expert technical assistance in larval behavior; Jazmine Ottley and Konstantin Fishilevich for assistance in larval behavior; Helen Shio of the Rockefeller University BioImaging Facility for performing the electron microscopy; Mayte Farinas for advice on statistics; an anonymous reviewer who provided valuable input on the statistical approach in an earlier version of this paper; Joel E. Cohen for extensive discussions on the statistical approach; and Richard Axel, Cori Bargmann, Larry Katz, Kevin Lee, Kristin Scott, and members of the Vosshall lab for comments on the manuscript. Author contributions were as follows: E.F. constructed and analyzed the *OR*-Gal4 lines and participated in the FDR analysis of behavioral data; A.I.D. established the behavioral assay, oversaw the collection of data, and carried out initial data analysis with F.N.; K.A. carried out the in situ hybridization; F.N. advised on the statistical analysis of the data; L.B.V. advised in the design and interpretation of the experiments and wrote the paper; and M.L. supervised part of the data collection and designed and carried out the FDR analysis of the entire behavioral dataset as well as the linear regression model. This work was supported by grants to L.B.V. from the National Science Foundation (IBN-0092693); the National Institutes of Health (R01 DC005036 and RO1 DC006711); and the McKnight, Beckman, and John Merck Foundations. E.F. is supported by an NIH/Ruth L. Kirschstein NRSA (F31 DC006795) predoctoral fellowship. A.I.D. is a Gulbenkian predoctoral fellow (PGDBM) supported by an FCT fellowship. M.L. is a postdoctoral fellow of the Belgian-American Educational Foundation. F.N. is supported by a Bristol-Myers Squibb fellowship and the Swiss NCCR program in Molecular Oncology.

Received: October 20, 2005
Revised: November 4, 2005
Accepted: November 7, 2005
Published: December 5, 2005

References

1. Mombaerts, P. (1999). Seven-transmembrane proteins as odorant and chemosensory receptors. Science *286*, 707–711.
2. Malnic, B., Hirono, J., Sato, T., and Buck, L.B. (1999). Combinatorial receptor codes for odors. Cell *96*, 713–723.
3. Touhara, K., Sengoku, S., Inaki, K., Tsuboi, A., Hirono, J., Sato, T., Sakano, H., and Haga, T. (1999). Functional identification and reconstitution of an odorant receptor in single olfactory neurons. Proc. Natl. Acad. Sci. USA *96*, 4040–4045.
4. Araneda, R.C., Kini, A.D., and Firestein, S. (2000). The molecular receptive range of an odorant receptor. Nat. Neurosci. *3*, 1248–1255.
5. Hallem, E.A., Ho, M.G., and Carlson, J.R. (2004). The molecular basis of odor coding in the *Drosophila* antenna. Cell *117*, 965–979.
6. Rodrigues, V. (1988). Spatial coding of olfactory information in the antennal lobe of *Drosophila melanogaster*. Brain Res. *453*, 299–307.
7. Johnson, B.A., Woo, C.C., and Leon, M. (1998). Spatial coding of odorant features in the glomerular layer of the rat olfactory bulb. J. Comp. Neurol. *393*, 457–471.
8. Galizia, C.G., Sachse, S., Rappert, A., and Menzel, R. (1999). The glomerular code for odor representation is species specific in the honeybee *Apis mellifera*. Nat. Neurosci. *2*, 473–478.
9. Wachowiak, M., and Cohen, L.B. (2001). Representation of odorants by receptor neuron input to the mouse olfactory bulb. Neuron *32*, 723–735.
10. Belluscio, L., and Katz, L.C. (2001). Symmetry, stereotypy, and topography of odorant representations in mouse olfactory bulbs. J. Neurosci. *21*, 2113–2122.
11. Wang, J.W., Wong, A.M., Flores, J., Vosshall, L.B., and Axel, R. (2003). Two-photon calcium imaging reveals an odor-evoked map of activity in the fly brain. Cell *112*, 271–282.
12. Tissot, M., Gendre, N., Hawken, A., Stortkuhl, K.F., and Stocker, R.F. (1997). Larval chemosensory projections and invasion of adult afferents in the antennal lobe of *Drosophila*. J. Neurobiol. *32*, 281–297.
13. Singh, R.N., and Singh, K. (1984). Fine structure of the sensory organs of *Drosophila melanogaster* Meigen larvae (*Diptera*: *Drosophilidae*). Int. J. Insect Morphol. Embryol. *13*, 255–273.
14. Larsson, M.C., Domingos, A.I., Jones, W.D., Chiappe, M.E., Amrein, H., and Vosshall, L.B. (2004). *Or83b* encodes a broadly expressed odorant receptor essential for *Drosophila* olfaction. Neuron *43*, 703–714.

15. Neuhaus, E.M., Gisselmann, G., Zhang, W., Dooley, R., Stoertkuhl, K., and Hatt, H. (2004). Odorant receptor heterodimerization in the olfactory system of *Drosophila melanogaster*. Nat. Neurosci. *8*, 15–17.
16. Kreher, S.A., Kwon, J.Y., and Carlson, J.R. (2005). The molecular basis of odor coding in the *Drosophila* larva. Neuron *46*, 445–456.
17. Couto, A., Alenius, M., and Dickson, B.J. (2005). Molecular, anatomical, and functional organization of the *Drosophila* olfactory system. Curr. Biol. *15*, 1535–1547.
18. Python, F., and Stocker, R.F. (2002). Adult-like complexity of the larval antennal lobe of *D. melanogaster* despite markedly low numbers of odorant receptor neurons. J. Comp. Neurol. *445*, 374–387.
19. Ramaekers, A., Magnenat, E., Marin, E.C., Gendre, N., Jefferis, G.S., Luo, L., and Stocker, R.F. (2005). Glomerular maps without cellular redundancy at successive levels of the *Drosophila* larval olfactory circuit. Curr. Biol. *15*, 982–992.
20. Ayyub, C., Paranjape, J., Rodrigues, V., and Siddiqi, O. (1990). Genetics of olfactory behavior in *Drosophila melanogaster*. J. Neurogenet. *6*, 243–262.
21. Monte, P., Woodard, C., Ayer, R., Lilly, M., Sun, H., and Carlson, J. (1989). Characterization of the larval olfactory response in *Drosophila* and its genetic basis. Behav. Genet. *19*, 267–283.
22. Cobb, M. (1999). What and how do maggots smell? Biological Reviews *74*, 425–459.
23. Oppliger, F.Y., Guerin, P.M., and Vlimant, M. (2000). Neurophysiological and behavioural evidence for an olfactory function for the dorsal organ and a gustatory one for the terminal organ in *Drosophila melanogaster* larvae. J. Insect Physiol. *46*, 135–144.
24. Dobritsa, A.A., van der Goes van Naters, W., Warr, C.G., Steinbrecht, R.A., and Carlson, J.R. (2003). Integrating the molecular and cellular basis of odor coding in the *Drosophila* antenna. Neuron *37*, 827–841.
25. Fishilevich, E., and Vosshall, L.B. (2005). Genetic and functional subdivision of the *Drosophila* antennal lobe. Curr. Biol. *15*, 1548–1553.
26. Goldman, A.L., van der Goes van Naters, W., Lessing, D., Warr, C.G., and Carlson, J.R. (2005). Coexpression of two functional odor receptors in one neuron. Neuron *45*, 661–666.
27. Brand, A.H., and Perrimon, N. (1993). Targeted gene expression as a means of altering cell fates and generating dominant phenotypes. Development *118*, 401–415.
28. Vosshall, L.B., Wong, A.M., and Axel, R. (2000). An olfactory sensory map in the fly brain. Cell *102*, 147–159.
29. Dunipace, L., Meister, S., McNealy, C., and Amrein, H. (2001). Spatially restricted expression of candidate taste receptors in the *Drosophila* gustatory system. Curr. Biol. *11*, 822–835.
30. Scott, K., Brady, R., Jr., Cravchik, A., Morozov, P., Rzhetsky, A., Zuker, C., and Axel, R. (2001). A chemosensory gene family encoding candidate gustatory and olfactory receptors in *Drosophila*. Cell *104*, 661–673.
31. Pino, J.A., Mesa, J., Munoz, Y., Marti, M.P., and Marbot, R. (2005). Volatile components from mango (Mangifera indica L.) cultivars. J. Agric. Food Chem. *53*, 2213–2223.
32. Argenta, L.C., Mattheis, J.P., Fan, X., and Finger, F.L. (2004). Production of volatile compounds by fuji apples following exposure to high CO_2 or low O_2. J. Agric. Food Chem. *52*, 5957–5963.
33. Idstein, H., Herres, W., and Schreier, P. (1984). High resolution gas chromatography mass spectrometry and gas chromatography Fourier transform IR analysis of Cherimoya *Annona cherimolia* volatiles. J. Agric. Food Chem. *32*, 383–389.
34. Jordan, M.J., Tandon, K., Shaw, P.E., and Goodner, K.L. (2001). Aromatic profile of aqueous banana essence and banana fruit by gas chromatography-mass spectrometry (GC-MS) and gas chromatography-olfactometry (GC-O). J. Agric. Food Chem. *49*, 4813–4817.
35. Stensmyr, M.C., Giordano, E., Balloi, A., Angioy, A.M., and Hansson, B.S. (2003). Novel natural ligands for *Drosophila* olfactory receptor neurones. J. Exp. Biol. *206*, 715–724.
36. Zhu, J., Park, K.-C., and Baker, T.C. (2003). Identification of odors from overripe mango that attract vinegar flies, *Drosophila melanogaster*. J. Chem. Ecol. *29*, 899–909.
37. Cobb, M., Bruneau, S., and Jallon, J.M. (1992). Genetic and developmental factors in the olfactory response of *Drosophila melanogaster* larvae to alcohols. Proc. R. Soc. Lond. B. Biol. Sci. *248*, 103–109.
38. Cobb, M., and Dannet, F. (1994). Multiple genetic control of acetate-induced olfactory responses in *Drosophila melanogaster* larvae. Heredity *73*, 444–455.
39. Bellen, H.J., D'Evelyn, D., Harvey, M., and Elledge, S.J. (1992). Isolation of temperature-sensitive diphtheria toxins in yeast and their effects on *Drosophila* cells. Development *114*, 787–796.
40. Han, D.D., Stein, D., and Stevens, L.M. (2000). Investigating the function of follicular subpopulations during *Drosophila* oogenesis through hormone-dependent enhancer-targeted cell ablation. Development *127*, 573–583.
41. Benton, R., Sachse, S., Michnick, S.W., and Vosshall, L.B. Atypical membrane topology and heteromeric function of *Drosophila* odorant receptors in vivo. PLoS Biol., in press.
42. Sokolowski, M.B. (1980). Foraging strategies of *Drosophila melanogaster*: A chromosomal analysis. Behav. Genet. *10*, 291–302.
43. Wu, Q., Wen, T., Lee, G., Park, J.H., Cai, H.N., and Shen, P. (2003). Developmental control of foraging and social behavior by the *Drosophila* neuropeptide Y-like system. Neuron *39*, 147–161.
44. Wilson, R.I., Turner, G.C., and Laurent, G. (2004). Transformation of olfactory representations in the *Drosophila* antennal lobe. Science *303*, 366–370.
45. Scherer, S., Stocker, R.F., and Gerber, B. (2003). Olfactory learning in individually assayed *Drosophila* larvae. Learn. Mem. *10*, 217–225.
46. Vosshall, L.B., Amrein, H., Morozov, P.S., Rzhetsky, A., and Axel, R. (1999). A spatial map of olfactory receptor expression in the *Drosophila* antenna. Cell *96*, 725–736.
47. Korn, E.L., Troendle, J.F., McShane, L.M., and Simon, R. (2004). Controlling the number of false discoveries: Application to high-dimensional genomic data. J. Stat. Plan. Inference *124*, 379–398.
48. Shaffer, J.P. (1995). Multiple hypothesis testing. Annu. Rev. Psychol. *46*, 561–584.
49. Zar, H.J. (1999). Biostatistical Analysis, 4th Edition, (Upper Saddle River: Prentice Hall).